http://dx.doi.org/10.21577/0100-4042.20170807 *Quim. Nova,* Vol. 45, No. 1, 74-82, 2022

Revisão

CHALLENGES OF TIO_2-COMPOSITE, AS A VISIBLE ACTIVE PHOTOCATALYST MATERIAL FOR SARS-COV-2 ANTIVIRAL COMPARED WITH THE OTHER VIRUSES

Diana Rakhmawaty Eddy[a,*], Muhamad Diki Permana[a], Annisa Lutfiah[a], Atiek Rostika Noviyanti[a], Yusi Deawati[a] and Iman Rahayu[a]

[a]Department of Chemistry, Universitas Padjadjaran, Jln. Raya Bandung-Sumedang Km. 21, Indonesia

Recebido em 05/04/2021; aceito em 16/07/2021; publicado na web em 13/08/2021

The efforts in dealing with COVID-19 in various aspects are continuously being carried out, such as the photocatalytic process. Interestingly, TiO_2 plays an important role as an environmentally friendly photocatalyst with a visible and UV absorption range. The increase in the antiviral performance of this compound is further maximized by formulating TiO_2-based composites and doping it to reduce the bandgap. This review aims to determine the challenges of TiO_2-based composite as a visible active photocatalyst material for SARS-CoV-2 antiviral. It presents a discussion of the photocatalytic function of TiO_2, by comparing the secondary data obtained from viruses that have been successfully degraded by the SARS-CoV-2. The literature search led to the analysis of the photocatalyst quality, structure, composition, and the degraded viruses. This comparison was based on the photocatalyst's general constituents, such as protein and RNA. The virus morphology as observed in the secondary data was successfully destroyed by hydroxyl radicals resulting from the photocatalytic processes. It was observed that TiO_2 photocatalyst generated ROS, capable of inactivating various viruses, therefore, it has the potential in fighting against the SARS-CoV-2. Moreover, further research is needed in photocatalyst design, its role, and the overall mechanism of virus inactivation.

Keywords: photocatalyst; COVID-19; virals inactivation; SAR-CoV-2.

INTRODUCTION

Currently, COVID-19 (Corona Virus Disease 19) is still a major problem in the world, causing various diseases, such as the respiratory illness with flu symptoms including coughing, fever, and difficult breathing caused by the Severe Acute Respiratory Syndrome Coronavirus 2 (SARS-CoV-2) virus.[1] Coronaviruses are small (65-125 nm in diameter) and contain single-stranded RNA as nucleic material, ranging in length from 26 to 32 kbs. Statistical data noted that some countries (especially developing nations) still have an increase in positive cases on a daily basis, which shows that this virus is easily transmitted. COVID-19 has mortality about 3-7%, compared to a death rate from influenza of less than 1%.[2]

Viruses are highly widespread microorganisms unable to survive without a host organism. Therefore, their survival depend on the virus-host dynamicity.[3] Viral contaminants which are associated with drinking water, breathable air, and food have become major threats, because of their effects on the environment and human health. Pathogens are transmitted through food, water, and air among individuals, causing infections and more than 15 million mortality globally per year.

The increase in the number of positive cases has a big impact on various parties, especially medical personnel. Besides airborne transmission, this virus is also transmitted by direct surface contact.[4,5] Moreover, there is a higher propensity for infections to follow an exposure to waterborne and airborne viruses, compared to other pathogenic microbial contaminants.[6,7] These infectious diseases are known to be widespread and majorly a health risk factor. The medical personnel are mostly at the forefront to interacting with patients, therefore, exposed to the risk of the infectious disease.

In addition, to reduce the occurrence of diseases caused by different viruses, various methods and ample efforts are utilized to disinfect pathogenic micro-organisms within the environment.[8,9] Waterborne viruses require several disinfection processes, including membrane filtration, ultraviolet (UV) treatment, and chemical disinfectants (ozone, chlorine dioxide, and chlorine).[10] However, there are several challenges faced in the implementation of these processes, including the production of hazardous byproducts, and this has limited the use of chemical disinfectants.[11] Nano and ultra-filtrations, as well as other membrane techniques, are efficient virus elimination methods, as a result of relatively small surface pore sizes, compared to viruses. However, the technique is inaccessible and energy consuming.[12] The UV method is expensive and also ineffective for highly illumination resistant virus.[13,14] The conventional methods for airborne virus disinfection include, thermal and non-thermal treatment, as well as UV light. These methods are not quite practical and effective, high cost and energy requirements.[15] Hence, there is a need to develop effective, affordable, environmentally friendly, reliable, low energy consumption, techniques for virus inactivation.

Photocatalysts are materials that convert light into chemical energy, and have been widely used in cleaning surfaces, air and water purification systems, sterilization, and photoelectrochemical conversion.[16] Zhang *et al.*[17] reported their usefulness in viral inactivation. One of the photocatalyst materials commonly used is titanium dioxide (TiO_2). The main advantages of this compound its high chemical stability in acidic and alkaline conditions, non-toxic, relatively low-cost, and safe oxidizer for the environment. These advantages makes TiO_2 a potential source for many photocatalytic applications,[18] and the best choice in bringing out antiviral properties. However, according to Lee *et al.*[19] this compound has limited photocatalytic efficiency due to its wide band energy gap, such as in anatase TiO_2 (3.2 eV), which is in the ultraviolet wavelength range. This is a disadvantage of using it in photocatalysis, and also, the required ultraviolet light reduces its efficiency because UV rays are relatively dangerous.

Metal-TiO_2 composites are preferred because they have the capacity to absorb light into the visible area and increase

*e-mail: diana.rahmawati@unpad.ac.id

photocatalytic efficiency.[20] The use of visible light is more significant compared to UV, because 43% of the sun spectrum is within this range. Therefore, successfully manufacturing photocatalysts in the presence visible light is an important problem in this field. Gold (Au) has a suitable band-gap, and is as a result, the most suitable element for this process. The nano-plasmonic Au applied on the TiO_2 surface has a double effect of being able to operate effectively in the visible spectrum range and exhibit strong localized surface plasmon resonance (LSPR). In addition, nano-Au acts as an electron trap, therefore, reducing the occurrence of electron-hole recombination.[21] Chowdhury *et al*.[20] composited TiO_2 with gold nanoparticles, resulting in the lowest bandgap and maximum photocatalytic efficiency during phenol degradation.

In addition, there are several comprehensive evaluations estimated to summarize photocatalysis disinfection method on microorganisms, including fungi, bacteria, algae, viruses and protozoa.[21] The results obtained tend to not have a specific translation into the potential disinfection of SARS-CoV-2 type virus, characterized by a unique persistence, composition, and structure. In addition, there have been advancements in virus detection methods alongside increased public health concerns on this virus. Therefore, it is essential to obtain a better understanding of photocatalytic disinfection, for application as a robust, effective and sustainable strategy during COVID-19 prevention.

This review aims to explore the effects of photoactivated composite-TiO_2, as a visible active material for viruses. In addition, this study also reviews a wide range of photocatalysts used in viral disinfection, as well as the prospective strengths and weaknesses of the known active component, TiO_2, on SARS-CoV-2 virus. This is currently also the first systematic study of viral disinfection for SARS-CoV-2 virus, using photocatalysis.

RESULTS AND DISCUSSION

Photocatalytic of TiO_2

TiO_2 has been recognized as a photocatalyst in demand since the early 1970s.[22] Starting with the conversion of photoelectrochemical solar energy to other areas, such as environmental photocatalysis, hydrophilicity, self-cleaning, antifogging, and most recently as antimicrobials.[23] As a semiconductor, TiO_2 absorbs photons of sufficient energy to excite electrons (e^-) from the valence to the conduction band, and consequently, leaves a positively charged hole (h^+) in the valence band, as seen in Equation 1. Figure 1 shows the photocatalytic mechanism of TiO_2.[24] The bandgap energy of the anatase phase is about 3.2 eV. This indicates photocatalysis is activated by photons of wavelengths lower than 385 nm (UVA). The electrons and holes then recombine, or migrate to the surface before reacting, to produce reactive oxygen species (ROS), including $O_2^{-\bullet}$ (2) and ·OH (3).[25] Furthermore, radical reactions with organic compounds lead to mineralization,[20] while membrane lipids are facilitated by microbes,[21] and this recombination lowers process' efficiency. Research has developed composites as a method of reducing recombination.[25]

$$TiO_2 + h\nu \rightarrow e^- + h^+ \quad (1)$$

$$O_2 + e^- \rightarrow O_2^{-\bullet} \quad (2)$$

$$h^+ + H_2O \rightarrow {}^{\bullet}OH + H^+ \quad (3)$$

Only photons with energies above the band-gap (ΔE) produce electron excitation and encourage reaction to occur.[26] Photons absorption with energies less than ΔE or longer wavelengths, often lead to the emission of heat energy. Also, the minimum wavelength required to promote an electron is dependent on the photocatalyst's band gap energy. This equation is given below:[27]

$$E = 1240/\lambda \quad (4)$$

where λ is the wavelength of light, in nm.

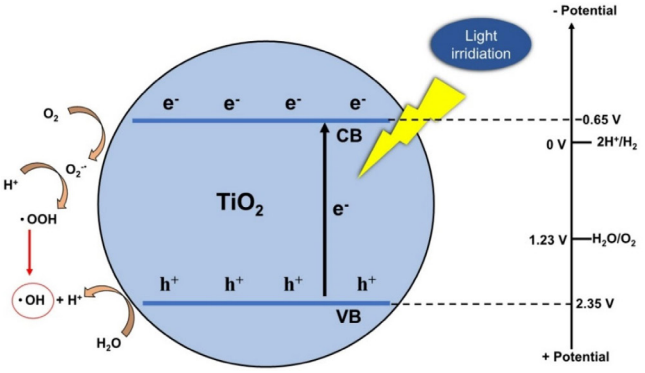

Figure 1. *A schematic diagram illustrating the photocatalytic principle of TiO_2*

TiO_2-composite, a visible active photocatalyst

In the application of TiO_2 for viral disinfection, some major challenges faced are the high rate of charge recombination between electrons and holes, and the reduction in photocatalytic performance. Another significant limitation observed is the wide band gap (3.0 eV and 3.2 eV for rutile and anatase phases, respectively). Therefore, the material is only effective in the presence UV irradiation, and this is approximately 4% of the total solar energy.[17] However, there have been considerable attempts to increase the photocatalyst's efficiency by reducing the rate of recombination and shifting the band gap energy towards the region of visible light, in a bid to improve solar energy utilization during disinfection of viral items or substances.

By using the blackbody radiation approach, the intensity of the sunlight in the wavelength range of 0-5 μm was estimated. Assuming that the sun's surface temperature is at 6,000 K, the intensity of the sunlight is calculated using the Plank function.[28]

$$B(T) = C_1 \int_{v}^{\infty} \{v^3[\exp(C_2 v / T) - 1]\} dv \quad (5)$$

where B(T) = radiance (in units of W cm^{-2} sr^{-1}), v = frequency (expressed as wavenumber per centimeter), T is absolute temperature in kelvins; C_1 = the first radiation constant (1.1909×10^{-12} W cm^2 sr^{-1}), and C_2 = the second radiation constant (1.438833 K cm). From Figure 2, the maximum intensity of sunlight is in the wavelength range of 300-600 nm (Figure 2b). Therefore, a photocatalyst that is active in visible light is used to make an efficient photocatalyst.

Several studies have developed TiO_2 to work on visible light, one of which is a composite. In addition to reducing the band gap, composites are also able to trap charges, thus, lowering the electron-hole rate of recombination. Figure 3 illustrates the effect of the composite on TiO_2's band gap. Several factors, including the composite type, concentration, and production technique, as well as the catalyst's physico-chemical properties, regulate the influence of photocatalytic activity on composites.[26] Table 1 shows the effect of composites on the bandgap of TiO_2 photocatalysts from various photocatalytic applications. Metal oxide is a material often used as a composite for photocatalysis. Bai *et al*.[29] composited TiO_2 with WO_3 and MoO_3 with different compositions using the sol-gel method.

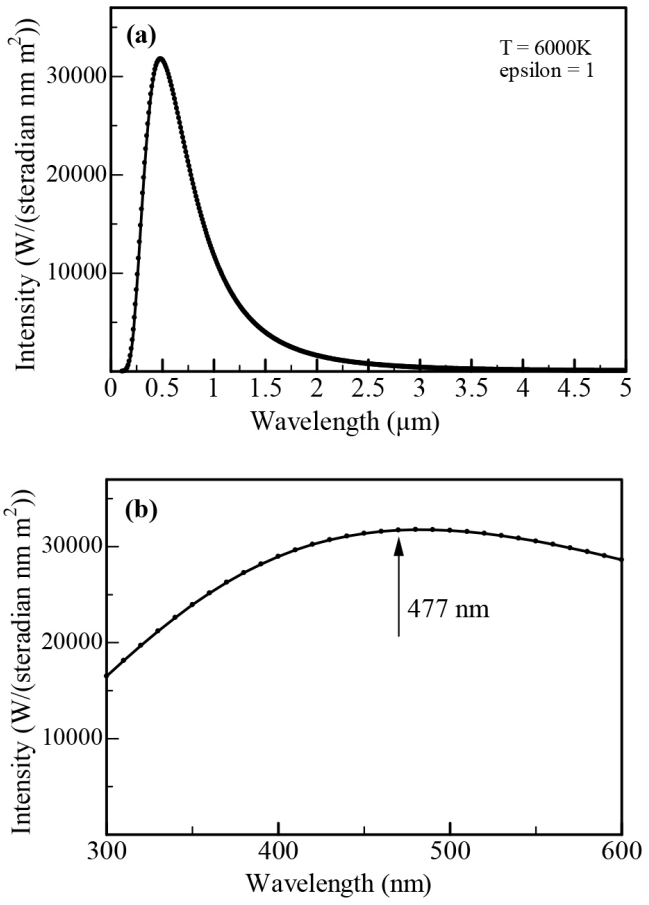

Figure 2. *The intensity of sunlight (6,000 K) using the blackbody radiation equation (a) 0-0.5 μm, (b) 0.3-0.6 μm*

The results showed the composites of 5 wt% WO_3/TiO_2 and 2 wt% MoO_3/TiO_2 degraded RhB optimally, under visible light. These conditions indicated a 5 wt% WO_3 and a 500°C calcination temperature for WO_3/TiO_2, while a 2 wt% MoO_3, and a calcination temperature of 300 °C, were denoted for the MoO_3/TiO_2 composites. The high photocatalytic activity obtained is as a result of the efficient separation of charge carriers. Thus, composites containing efficient metal oxides are potential options for notably increasing TiO_2's photocatalytic activity, in the presence of visible light.

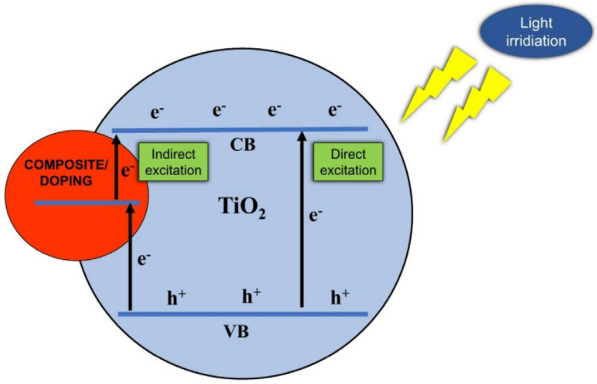

Figure 3. *Schematic diagram illustrating the principle of reducing the band gap of the composite photocatalyst on TiO_2*

Another composite (Cu_2O) was also reported by Jiang *et al.*[30] to reduce the band gap to 2.00 eV. Cu_2O/TiO_2 composites were created without templates or additives, through an unsophisticated hydrothermal method, by reacting $Cu(CH_3COO)_2{\cdot}H_2O$, with $(NH_4)_2TiF_6$. Therefore, the photo-degradation potential of methylene blue (MB) solution under visible light is evaluated to estimate the photocatalytic activity. In contrast with pure TiO_2, the composite's UV-Vis absorption spectra demonstrated a redshift within the band-gap transition. This property was observed between the visible region and absorption edge and attributed to the Cu_2O content. Furthermore, the research of Munoz-Batista *et al.*[31] used CeO_2 as a composite of TiO_2, which was obtained by the microemulsion method followed by calcination. Using this sample as a photocatalyst, mineralization of toluene and the inactivation of *Escherichia coli* 1337-H were carried out under UV and visible illumination conditions.

Liu *et al.*[32] investigated the effect of Bi_2O_3 composites on TiO_2. Bi_2O_3/TiO_2 photocatalysts, which was prepared using the sol-gel method without water through various Bi-Ti atomic ratios and calcination temperatures. The results showed that the Bi_2O_3/TiO_2 photocatalyst with a 1.75% Bi-Ti proportion exhibited the best performance during methyl orange (MO) degradation. Furthermore, the photocatalytic degradation rate of MO reduced gradually with increasing calcination from 420-620°C. Other advantages of the Bi_2O_3 composite are the effective suppression of the anatase phase transformation to rutile, prevent crystal overgrowth, and increase the absorption of visible light compared to the pure TiO_2.

In other studies, carbon compounds have also been used in photocatalytic composites. Khalid *et al.*[33] used graphene as a TiO_2 composite. This material was synthesized through hydrothermal techniques, and the results indicated a shift in the TiO_2 absorption edge towards the visible light region, following a consequent increase in the total graphene present. In addition, efficient methyl orange (MO) photodegradation was observed with the graphene/TiO_2 composites, and this was greater in the presence of visible light, compared to pure TiO_2 samples. This is due to the extended range of light absorption, significant absorbency of dye, and the efficient charge separation as a result of the planar two-dimensional structure of graphene. Wang *et al.*,[34] composited multi-walled carbon nanotubes (MWNT) with a TiO_2 composite catalyst, produced using a modified sol-gel technique, for phenol degradation. The results indicated increasing the MWNT/TiO_2 ratio from 5 to 20% supports an increased synergistic effect on phenol loss, which is correlated with changes in the UV-vis solid spectrum.

Inactivation of viruses by photocatalyst of TiO_2

Photocatalysis inactivate a wide variety of organisms including bacteria, endospores, fungi, algae, protozoa, viruses, and prions.[21] Waterborne viruses such as phage MS2, bacteriophage, and phage f2 are disinfected using TiO_2 photocatalysts, resulting to 1.8-log to 6-log in a time span of 2 to 180 min.[15,53-55] Airborne viruses produced in 4-log disinfection efficiency, until they are eliminated in a susceptible short irrigation time up to 7 min.[56,57] Foodborne viruses, such as MNV-1 resulted in a 3.2-log to> 5.5-log disinfection efficiency in the range of 109 to 160 min.[58,59] There was a positive response to virus reduction based on the disinfection efficiency, which is influenced by the radicals generated based on the band gap size of the photocatalyst. Some examples of different viral inactivation using photocatalysts are shown in Table 2.

Effect of parameters on viral degradation

Several parameters that determine the photocatalyst performance in degrading viruses include the type of virus, light source, and catalyst concentration.

Table 1. Effect of composites on the TiO_2 photocatalyst band gap

Photocatalyst	Composite (%)	Optimum composite (%)	Wavelength (nm)	Band gap (eV)	Ref.
In_2S_3/TiO_2	20-60	40	580	2.14	35
Bi_2WO_6/TiO_2	5-20	15	405	3.06	36
Fe/TiO_2	0.4-4.9	1.1	411	3.02	37
$NdPW_{12}O_{40}/TiO_2$	0-10	1.0	350	3.54	38
WO_3/TiO_2	2-20	5	Visible	-	29
MoO_3/TiO_2	2-20	2	Visible	-	29
$Graphene/TiO_2$	1-10	10	413	3.00	33
Cu_2O/TiO_2	-	-	620	2.00	30
CdS/TiO_2	1-4	-	550	2.25	39
$ZnFe_2O_4/TiO_2$	-	-	588	2.10	40
CeO_2/TiO_2	1-25	5	413	3.00	31
$Bi_2Ti_2O_7/TiO_2$	-	-	496	2.50	41
Bi_2O_3/TiO_2	0-2.34	1.75	435	2.85	32
SiC/TiO_2	1-10	5	502	2.47	42
PbS/Graphene/ TiO_2	0-0.2	0.2	~620	~2.00	43
CeF_3/TiO_2	-	0.2	524	2.37	44
$g\text{-}C_3N_4/TiO_2$	4-48	24	450	2.75	45
$CsPbBr_3/TiO_2$	-	-	530	2.34	46
$ZnO/Graphene/TiO_2$	-	-	441	2.81	47
Ag_3PO_4/TiO_2	4-14	12	506	2.45	48
$Chitosan/TiO_2$	-	-	Visible	-	49
$MgFe_2O_4/TiO_2$	0.5-5	2	Visible	-	50
$Au_{25}(SR)_{18}/TiO_2$	-	0.94	4.77	2.60	51
RuO_2/TiO_2	-	-	3.85	3.22	52
$MWNT/TiO_2$	5-40	20	Visible	-	34

Table 2. Summary of photocatalysts for virus inactivation

Photocatalyst	Light source	Virus	Time	Reduction	Ref.
TiO_2/polylysine (PL)-DNA	-	influenza A viruses	4 h	10^{-1} to 10^{-8}	60
Anatase nano TiO_2	UV light	H9N2 avian influenza virus	2.5 h	10^4 to 10^2 (99%)	61
Ag/TiO_2	UV light	PEDV	16 h	99.99%	62
		TGEV	16 h	99.99%	
N-doped TiO_2	280–700 nm	MS2 bacteriophage	2 h	4.5±0.2 log	63
UV-assisted TiO_2	254 nm	The murine norovirus	10 min	0.3 and 1.2 log_{10}	64
TiO_2 P25/$FeSO_4$	UV light	Phage MS2	10 min	6×10^4 to 4×10^0	54
TiO_2 film	UV light	influenza virus	8 h	4-log10	65
	Vis light	Odelia	24 h	1.50 log_{10}	66
	Vis light	SA11	24 h	2.78 log_{10}	
	Vis light	HAstV-1	24 h	2.42 log_{10}	
	Vis light	FCV	24 h	1.95 log_{10}	
	UV light	Herpes simplex virus	6 h	100%	67
TiO_2 P25	UV light	Murine Norovirus	4.6 min	3.6-log_{10}	68
	UV light	Phage MS2	65 min	2.8-log	69
	UV light	Hepatitis B virus	1 h	97%	70
	UV light	Poliovirus I	1 h	3-log	71
	UV light	Phage Qβ	2 min	3.5-log	65
SiO_2/TiO_2	UV light	Phage MS2	1.8 min	5-log	72
	UV light	Phage MS2	0.75 min	4.5-log	73
Cu/TiO_2 nanofibers	Vis light	Phage f2	4 h	5-log	74
Mn/TiO_2	Vis light	Phage MS2	1 h	4-log	75
TiO_2 nanoparticles	UV light	Influenza virus	5 h	9.5 to 4.5	76
	UV/Vis	SARS-CoV	6 h	99.99%	77

Virus Types

Different types of viruses affect the photocatalyst performance in degrading the pathogenic microbial. Each virus has different resistance influenced by size, shape, composition, and structure. Furthermore, the viral environment also influences viral resistance, such as waterborne and airborne viruses. Several types of viruses that have been tested for degradation are those infecting humans, such as influenza A,[60] H9N2 avian influenza,[61] Hepatitis B,[70] Herpes simplex virus,[67] and Poliovirus I.[71] Other viruses, such as SA11, FCV,[66] and Murine Norovirus[68] are examples of animal-infecting types that have also been investigated. Furthermore, the commonly used virus models are MS2[63] and Qß bacteriophages,[69] which are

bacteria-infecting, because they do not become pathogens in humans and easily reproduce. It has also been investigated that Ag/TiO_2 photocatalysts degrade up to 99.99% porcine epidemic diarrhea virus (PEDV) and transmissible gastroenteritis virus (TGEV),[62] which are pig-infecting coronavirus, is related to SARS-CoV-2, especially their similarity in organelle structure. Therefore, comparative analysis of degradation is better observed.

The comparison of the virus parameters is carried out using the same photocatalyst to degrade different viruses. TiO_2 photocatalysts were investigated regarding their use for the inactivation of Murine Norovirus (animal infecting),[68] Phage MS2,[54,78] phage Qβ (bacterial infectious),[69] Hepatitis B virus,[70] and Poliovirus I (human infectious).[71] The inactivate of the hepatitis B virus takes the longest time (240 min). Meanwhile, murine norovirus was able to be inactivated at a very short time of susceptibility (4.6 min). The results showed that the order of resistance was Hepatitis B virus > Phage MS2 > Poliovirus I > phage Qβ > Murine Norovirus.[68,70] These results indicated that there was no correlation between viral resistance to the type of host cell it infects. This comparison was carried out by UV irradiation of TiO_2. The UV light source given to the TiO_2 photocatalyst is an energy source used to produce radical species to degrade viruses.

The degradation experiments were carried out on two types of viruses with close ties, namely porcine epidemic diarrhea virus (PEDV) and transmissible gastroenteritis virus (TGEV), investigated with a degrading photocatalyst namely Ag/TiO_2.[62] Both viruses were treated the same by irrigation with UV light, having the same inactivation time of 16 hours with reduced power of 99.99%. From these data, it is assumed that the inactivation performance of photocatalysts in both bacteria with high similarities (structure and composition), produce the same inactivation power. This is closely related to the photocatalyst mechanism in the form of oxidative stress in the presence of radical species,[10] and does not depend on the details of mutations in viruses with close kinship. Based on these data, tracing the effect of virus on the photocatalyst process needs to be carried out in more detailed form. This further explain the effect of both structure and composition in the form of proteins and genes correlating with the inactivation of the virus by the photocatalytic process.

Light Source

Zan *et al.*[70] has investigated the photocatalytic effect of TiO_2 nanoparticles and TiO_2-coated ceramic plate on the surface antigen of Hepatitis B virus. The results showed that TiO_2 (0.5 g L^{-1}) degraded most of the of Hepatitis B virus under mercury lamp irradiation, with a light intensity of 0.05 mW/cm^2 at a wavelength of 365 nm or in room sunlight for several hours. TiO_2-coated ceramic plate has a stronger shutdown efficiency even under daylight irradiation in poorly lit rooms.

A study by Lee *at al.*[69] evaluated the UV irradiation disinfection ability at 254 nm wavelength compared to treatments in combination with titanium dioxide (TiO_2). In addition, the Qβ bacteriophage was adopted as a viral model, while TiO_2 suspension irradiation involved UV light with 254 nm intensity and 0.4 mW cm^{-2}. This combination approach is estimated to be more effective in Qß deactivation. Therefore, 3.5-log10 Qβ inactivation required TiO_2 suspension (10^3 mg L^{-1}) irradiation after illuminating for 2 min, while 2-log10 was deactivated while using UV alone.

In another study, to be able to inactivate the virus using visible light, TiO_2 photocatalysts were composited with metals. Venieri *et al.*[75] investigated the degree of inactivation of MS2 bacteriophages, induced by solar radiation using a TiO_2 catalyst with metal composites. The results showed that the TiO_2 metal composite caused a fairly large narrow bandgap and an extended spectral response to the visible light region. Then, the reduction of the MS2 phage population reached a level of 99.9% in the waste sample under solar irradiation, which was simulated within 60 min in the presence of a prepared metal composite catalyst. A longer exposure period is required in cases where natural sunlight radiation is inhibited to completely remove phages. Therefore, the metal composite catalyst tested showed very sensitive properties in the absence of UV rays. The activity of visible light include as catalyst, and is also useful in delaying electron hole pair recombination, to obtain a better explanation for metal composite titania properties.

Virus inactivation mechanism

Figure 4 shows the three different mechanisms proposed for rendering viruses inactive through TiO_2 photocatalysis. These are protein oxidation, shape distortion, as well as RNA damage from reactive oxygen species (ROSs) and h^+ from photocatalysts.[10] A study by Lee *et al.*[69] investigated the mechanism of inactivation of the Qβ bacteriophage in titanium dioxide suspension, in the presence of UV light supplied at a wavelength of 254 nm. The data obtained from combined RT-PCR amplification as well as MPN test showed the decrease in the MPN-PCR value implied the phage nucleic acid had possibly been damaged by hydroxyl radicals.

Furthermore, Mazurkova *et al.*[76] reported titanium dioxide in suspension form or absorbed on film, was able to destroy influenza-causing viruses after incubation for 30 minutes. Virological studies also showed TiO_2 was able to render influenza virus inactive. However, this depends on the incubation time as well as the nanoparticle concentration. This inactivation effect occurred in cases where incubation was carried out in the dark, as opposed to TiO_2 suspension. Therefore, the virus inactivation properties of TiO_2 are majorly as a result of direct contact between the virus and the nanoparticles.

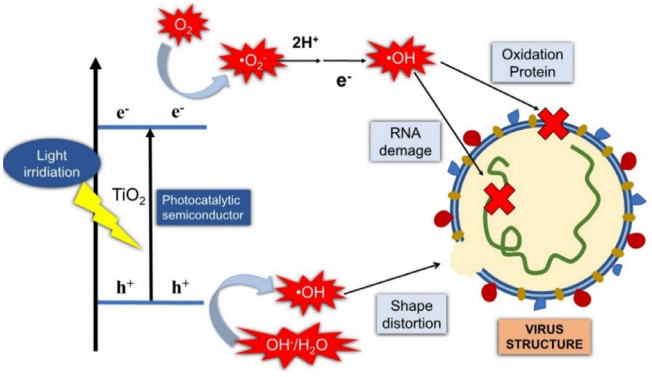

Figure 4. *Proposed mechanisms of viral disinfection, including shape distortion, protein oxidation, and RNA damage*

The photocatalysis reaction applied with TiO_2 to generate ROS demonstrated the ability to effectively exterminate numerous organisms. These include the endospore bacteria present in air water, and also on surfaces. In addition the technology is capable of providing a formidable weapon required to inhibit the transmission of infectious diseases, particularly in terms of developing visible light activated catalysts.[21] The mechanism of viral radical scavenging (strong oxidation-reducing power) which generally produces hydroxyl radicals (·OH), is disinfected using TiO_2 composite photocatalysts, such as visible light or sunlight to inactivate SARS-CoV-2 viruses.[79]

TiO_2 photocatalyst for SARS-CoV-2 antiviral

SARS-CoV-2 is a single-stranded RNA virus classified in the Coronaviridae family.[80] Although its exact size of has not been

reported, its diameter is approximately 82-94 nm, with spikes extending ~19 nm (total diameter ~120-132 nm).[81] SARS-CoV-2 is a beta coronavirus, with a viral genus enveloped in linear, positive sense, single-strand RNA genomes encoding four major structural proteins: envelope (E), membrane (M), spike (S), and nucleocapsid (N).[82] Figure 5 shows the schematic general structure of SARS-CoV-2, which is similar to other viral envelopes, consisting of the lipid bilayer and the nucleocapsid (the protein capsid that encloses the genome strand).[83] Therefore, it is possible to compare the performance of the photocatalyst degradation in other viruses.

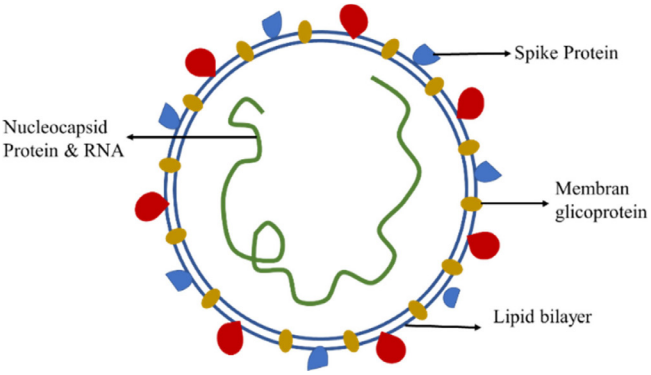

Figure 5. *Schematic general structure of SARS-CoV-2*

TiO_2 treatment to degrade rotavirus has shown that the product of reactive oxygen species (ROS), interacts with the viral protein membrane in the process of inactivation.[66] Rotavirus is a three-layered particle containing 11 segments of double-stranded RNA (ds) as its genome. RNA segments encode 6 structural (VP1-VP4, VP6, VP7) and 5-6 non-structural proteins (NSP1-NSP5/6).[84] Figure 6 shows the schematic structure of rotavirus.

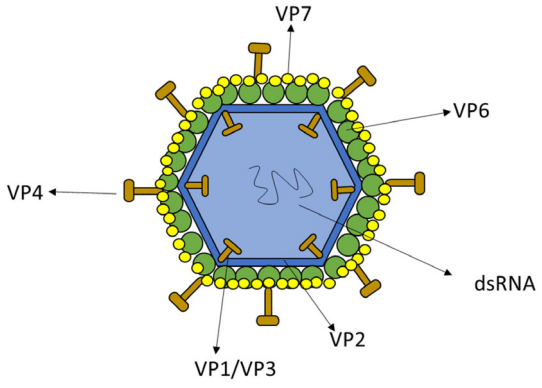

Figure 6. *Structure of rotavirus*[84]

Sang *et al.*[66] carried out a study on TiO_2 activation using white fluorescent lamps. The ROSs, including hydroxyl radicals (·OH) and superoxide anions ($\cdot O^{2-}$), were produced in significant quantity after stimulation had been carried out for 8, 16, and 24 hours. The inactivation of astrovirus, rotavirus, and FCV in the presence of TiO_2 films under visible light, showed their performance and mechanism. Other studies have explained that titanium dioxide destroys influenza viruses after 30 min of incubation. However, does not explain the effects of oxygen radicals virologically. This shows TiO_2's ability to inactivate influenza viruses, is dependent on the incubation period and the nanoparticles concentration.[76,85] Figure 7 illustrates the influenza virus' structure.

The activity performance of TiO_2 against the phage MS2 virus was investigated. The MS2 virion comprises three components: protein A

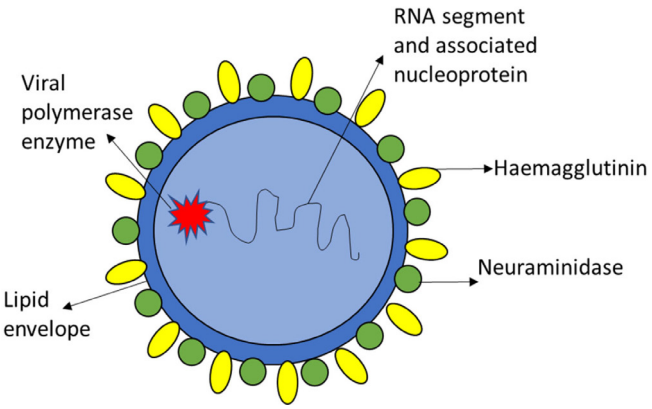

Figure 7. *Structure of influenza virus*[86]

(relative molecular weight Mr = 44,000), coat protein (relative molecular weight Mr = 13,700), and the single strand RNA molecules. The three-intact virons' three dimensional structure was ascertained and refined under a 2.8 Å resolution.[87] Meanwhile, the MS2 viruses successful degraded were about 60% of the phage population. This decline was observed after about 60 minutes of simulated solar radiation, at using MS2 viruses, at an initial concentration of 105 PFU mL^{-1}. Furthermore, the catalyst with binary dopants, showed the highest photocatalytic activity in all the experiments, as about 99% of the viruses, were degraded under 20 minutes of exposure. This confirms the composite dopants are able to produce a synergistic effect.[75]

Other findings suggested that TiO_2 photocatalysis significantly inactivate influenza viruses by reducing viral proteins with a degradation process that is influenced by UV-A intensity and exposure time. This effective inactivation occurs below the level of environmental UV-A intensity. The optimal method for evaluating the photocatalytic inactivation of the influenza virus by modifying the ISO model is obtained in the process.[65,88]

The degradation of Qβ bacteriophages by titanium dioxide (TiO_2) with UV irradiation alone was carried out successfully. The process of viral inactivation explains the phage damage of nucleic acid Qß, resulting from the photocatalysis-induced radical oxidation. In addition, MPN-PCR denotes potential oxidative damage to the nucleic acid phages through the impact of hydroxyl radicals.[69] Xu *et al.*[89] acknowledged the effects of TiO_2 on hepatitis B virus (HBV), and the degradation outcome was predominantly attributed to the destruction of hepatitis B surface antigen (HBsAg), casein and RNA through oxidative photocatalysis. The TiO_2 was estimated to destroy a majority while using weak irradiation, or exposure to indoor sunlight for several hours. Moreover, stronger levels are essential in experiments with suspension, compared to ceramic plates coated with TiO_2. Therefore, the usefulness is expressed as an effective sterilizer with HBV inactivation capacity through photocatalysis.[70] SARS-CoV-2 is a large, enveloped, positive-stranded RNA virus, with a nucleocapsid and a structure similar to SARS-CoV-1, as well as a diameter that ranges from 80 to 140 nm.[90] Investigations were carried out on the SARS-CoV virus inactivated by TiO_2 apatite with a degradation of 99.99%, after irrigation for 6 hours under non-UV irradiation conditions. However, under UV irradiation conditions, the photocatalytic titanium apatite (PTAF) filter was able to completely deactivate/decompose SARS CoV.

This study has provided the first evidence that PTAF inactivate the SARS-CoV virus, which suggests that this material should be applied to the prevention of pathogenic microbial. SARS-CoV has 80% similarity with SARS-CoV-2. The results obtained in the assumption that modified TiO_2 is capable of being a good degradation candidate,[77]

indicated the parts damaged parts of SAR-CoV-2 virus, namely cell membranes, protein spikes, and damage RNA.[17]

Plasma membrane

The mechanism of inactivation vary between different viruses. Based on Table 2, the types of viruses were successfully degraded and inactivated by TiO_2 photocatalysts. Furthermore, the mechanism involved in the cell wall and cytoplasmic membrane inactivation were as a result of reactive oxygen species generation.[21] Generally, the plasma membrane comprises of amphipathic glycolipids, and phospholipid bilayer. These are crossed by various trans-membrane glycoprotein and polypeptide molecules. The carbohydrates from glycoproteins occur as oligosaccharide branches, and are often attached to the nitrogen end of the polypeptide, protruding from the outside.[91] In addition, the cell membrane is the outmost cell part, responsible for protecting viral cell formation, transporting materials and signaling.[92] Meanwhile, the lipid bilayer is predisposed to chemical disturbance, for instance, the interference of surfactants with the lipid envelope leads to inactivation of the virus.[93]

Viral disinfections are generally as more complex, compared to first-order profiles, and this is typically observed during the photocatalytic degradation of chemical pollutants. This is due to the ambiguous relationship between the virus' viability and chemical structure at the end of oxidation, and also because of the virus' complex, unclear repair mechanisms. Hence, organic photocatalytic degradation was concluded to be part of the viral disinfection process.[17]

Reactive oxygen species (ROS) are the natural byproducts of breathing organisms metabolism. The small amounts of ROS is controlled by cellular antioxidant defenses, such as the glutathione/glutathione disulfide (GSH/GSSG) ratio, however, its excess result in oxidative stress.[94] TiO_2 photocatalyst generates additional free radicals which attacks membrane lipids and cause damage.[95] Furthermore, photocatalysts also cause physical damage to the viral structures with sharp edges on the nanostructures,[96] and the loaded metal ions are toxic to the virus.[73]

Spike protein

The spike protein has an important role in SAR-CoV-2 virus infection in the host cells. The virus enters the host cells in the presence of angiotensin converting enzyme 2 (ACE2), which is found in the lungs, and uses a protein spike to bind ACE2.[90] Photocatalysts play a role in producing radical species to oxidize proteins and cause oxidative stress. The presence of radical species cause damage to the organelles that make up the protein.

Furthermore, the exposure of proteins to ROS at the cellular level, has been known to alter the side chains of amino acid, and consequently, alter the amino acids structures.[97] The destruction of viral proteins is mostly observed in the spike protruding from the sheath and other parts (i.e. envelope (E) and membrane (M)). Also, protein damage repair is limited to reduction of the oxidized sulfur-containing amino acid residue derivatives. Meanwhile, no other protein oxidation improvement were reported.[96]

RNA

Free radicals are known to attack bases and parts of RNA sugars, resulting in lesions, such as the breakdown of single and double strands, changes in bases and sugars, and cross-links to other molecules blocking RNA replication.[98] Li *et al*.[99] also investigated the influence of ROS on MS2 virus gene defects. This damage is then assessed using the reverse transcription polymerase chain reaction (RT-PCR), or the real-time quantitative polymerase chain reaction (qRT-PCR), or even when the virus surface protein is intact, damage on the genes restrain its reproduction in infected host cells, therefore, inactivating the pathogenic microbe.

CONCLUSIONS

The materials that are used in forming composites with TiO_2 which reduce its band gap, are recommended as active photocatalysts with the exposure to visible or sunlight (Table 1). TiO_2 composite photocatalysts produce ROS capable of killing various viruses (Table 2). This technology is potentially used as an effective weapon while fighting infectious disease transmission, including COVID-19.

Therefore, further research in the field of photocatalysis and viral disinfection is a challenge, expected to serve as an opportunity. In addition, emphasis ought to be placed on applied study approaches using photocatalyst design to achieve SARS-CoV-2 virus disinfection. Also, understanding the various inactivation mechanism, comprising viral responses and the role of photocatalytic materials is considered essential.

ACKNOWLEDGEMENTS

The authors are grateful to the Universitas Padjadjaran with The Riset Data Pustaka dan Daring (RDPD) Grant, Number: 1735/UN6.3.1/LT/2020 for supporting financially.

REFERENCES

1. https://www.who.int/publications-detail/disease-commodity-package---novel-coronavirus-(ncov), accessed April 2020.
2. Lai, C. C.; Shih, T. P., Ko, W. C.; Tang, H. J.; Hsueh, P. R.; *Int. J. Antimicrob. Agents*. **2020**, *55*, 105924.
3. Moelling, K.; *Electroanalysis* **2020**, *32*, 669.
4. Cesewski, E.; Johnsson, B. N.; *Biosens. Bioelectron*. **2020**, *159*, 112214.
5. El-Sayed, A.; Kamel, M.; *Environ. Sci. Pollut. Res*. **2020**, *27*, 19200.
6. Yates, M. V.; *Manual of environmental microbiology*, 4th Ed., John Wiley & Sons: New York, 2016.
7. Xie, M.; Chen, Q.; *Int. J. Infect. Dis.* **2020**, *94*, 119.
8. Ren, H.; Koshy, P.; Chen, W. F.; Qi, S.; Sorell, C. C.; *J. Hazard. Mater.* **2017**, *325*, 340.
9. Ateia, M.; Alalm, M. G.; Awfa, D.; Johnson, M. S.; Yoshimura, C.; *Sci. Total Environ*. **2020**, *698*, 134197.
10. Zhang, C.; Li, Y.; Shuai, D.; Shen, Y.; Xiong, W.; Wang, L.; *Chemosphere* **2019**, *214*, 462.
11. Cedergren, M. I.; Selbing, A. J.; Lofman, O.; Kallen, B. A.; *Environ. Res*. **2002**, *89*, 124.
12. Zhang, C.; Zhang, M.; Li, Y.; Shuai, D.; *Appl. Catal., B* **2019**, *248*, 11.
13. Hijnen, W. A. M.; Beerendonk, E. F.; Medema, G. J.; *Water Res*. **2006**, *40*, 3.
14. Li, D.; Gu, A. Z.; He, M.; Shi, H. C.; Yang, W. U. V.; *Water Res*. **2009**, *43*, 3261.
15. Yu, B. F.; Hu, Z. B.; Liu, M.; Yang, H. L.; Kong, Q. X.; Liu, Y. H.; *Int. J. Refrig*. **2009**, *32*, 3.
16. Nakataa, K.; Fujishima, A.; *J. Photochem. Photobiol., C* **2012**, *13*, 169.
17. Zhang, C.; Li, Y.; Shuai, D.; Shen, Y.; Wang, D.; *Chem. Eng. J*. **2019**, *355*, 399.
18. Eddy, D. R.; Rahayu, I.; Wyantuti, S.; Hartati, Y. W.; Firdaus, M. L.; Bahti, H. H.; *J. Phys.: Conf. Ser*. **2018**, *1080*, 012013.
19. Lee, M. S.; Hong, S. S.; Mohseni, M.; *J. Mol. Catal. A: Chem*. **2005**, *242*, 135.
20. Chowdhury, I. H.; Roy, M.; Kundu, S.; Naskar, M. K.; *J. Phys. Chem. Solids* **2019**, *129*, 329.
21. Foster, H. A.; Ditta, I. B.; Varghese, S.; Stelle, A.; *Appl. Microbiol. Biotechnol*. **2011**, *90*, 1847.

22. Fujishima, A.; Honda, K.; *Nature* **1972**, *238*, 37.
23. Fujishima, A.; Rao, T. N.; Tryk, D. A.; *J. Photochem. Photobiol., C* **2000**, *1*, 1.
24. Harper, J. C.; Christensen, P. A.; Egerton, T. A.; Curtis, T. P.; Gunlazuardi, J.; *J. Appl. Electrochem.* **2001**, *31*, 623.
25. Zheng, H.; Svengren, H.; Huang, Z.; Yang, Z.; Zou, X.; Johnsson, M.; *Microporous Mesoporous Mater*. **2018**, *264*, 147.
26. Ahmed, S.; Rasul, M. G.; Martens, W. N.; Brown, R.; Hashib, M. A.; *Desalination* **2010**, *261*, 3.
27. Mills, A.; Davies, R. H.; Worsley, D.; *Chem. Soc. Rev*. **1993**, *22*, 417.
28. Widger Jr, W. K.; Woodall, M. P.; *Bull. Am. Meteorol. Soc.* **1976**, *57*, 1217.
29. Bai, S.; Liu, H.; Sun, J.; Tian, Y.; Chen, S.; Song, J.; Luo, R.; Li, D.; Chen, A.; Liu, C. C.; *Appl. Surf. Sci*. **2015**, *338*, 61.
30. Jiang, G.; Wang, R.; Jin, H.; Wang, Y.; Sun, X.; Wang, S.; Wang, T.; *Powder Technol*. **2011**, *12*, 284.
31. Munoz-Batista, M. J.; Ferrer, M.; Fernandez-Garcia, M.; Kubacka, A.; *Appl. Catal., B* **2014**, *154*, 350.
32. Liu, Y.; Xin, F.; Wang, F.; Luo, S.; Yin, X.; *J. Alloys Compd.* **2010**, *498*, 179.
33. Khalid, N. R.; Ahmed, E.; Hong, Z.; Sana, L.; Ahmed, M.; *Curr. Appl. Phys.* **2013**, *13*, 659.
34. Wang, W.; Serp, P.; Kalck, P.; Faria, J. L.; *J. Mol. Catal. A: Chem*. **2005**, *235*, 194.
35. Gao, C.; Li, J.; Shan, Z.; Huang, F.; Shen, H.; *Mater. Chem. Phys*. **2010**, *122*, 183.
36. Du, Z.; Cheng, C.; Tan, L.; Lan, J.; Jiang, S.; Zhao, L.; Guo, R.; *Appl. Surf. Sci*. **2018**, *435*, 626.
37. Dholam, R.; Patel, N.; Adami, M.; Miotello, A.; *Int. J. Hydrogen Energy* **2009**, *34*, 5337.
38. Tiejun, C.; Ming, Y.; Xianwen, W.; Qian, D.; Zhenshan, P.; Wenhui, Z.; *Chin. J. Catal*. **2007**, *28*, 10.
39. Jang, J. S.; Kim, H. G.; Borse, P. H.; Lee, J. S.; *Int. J. Hydrogen Energy* **2007**, *32*, 4786.
40. Hou, Y.; Li, X. Y.; Zhao, Q. D.; Quan, X.; Chen, G. H.; *Adv. Funct. Mater*. **2010**, *20*, 2165.
41. Liu, H.; Chen, Y.; Tian, G.; Ren, Z.; Tian, C.; Fu, H.; *Langmuir* **2015**, *31*, 5962.
42. Li, Y.; Yu, Z.; Meng, J.; Li, Y.; *Int. J. Hydrogen Energy* **2013**, *38*, 3898.
43. Ullah, K.; Meng, Z. D.; Ye, S.; Zhu, L.; Oh, W. C.; *J. Ind. Eng. Chem*. **2014**, *20*, 1035.
44. Tang, C.; Hou, W.; Liu, E.; Hu, X.; Fan, J.; *J. Lumin*. **2014**, *154*, 305.
45. Tan, Y.; Shu, Z.; Zhou, J.; Li, T.; Wang, W.; Zhao, Z.; *Appl. Catal., B* **2018**, *230*, 260.
46. Schunemann, S.; Van Gastel, M.; Tuysuz, H.; *ChemSusChem* **2018**, *11*, 2057.
47. Nuengmatcha, P.; Chanthai, S.; Mahachai, R.; Oh, W. C.; *J. Environ. Chem. Eng*. **2016**, *4*, 2170.
48. Zhao, F. M.; Pan, L.; Wang, S.; Deng, Q.; Zou, J. J.; Wang, L.; Zhang, X.; *Appl. Surf. Sci*. **2014**, *317*, 833.
49. Zhang, X.; Xiao, G.; Wang, Y.; Zhao, Y.; Su, H.; Tan, T.; *Carbohydr. Polym*. **2017**, *169*, 101.
50. Zhang, L.; He, Y.; Wu, Y.; Wu, T.; *Mater. Sci. Eng. B*. **2011**, *176*, 1497.
51. Yu, C.; Li, G.; Kumar, S.; Kawasaki, H.; Jin, R.; *J. Phys. Chem. Lett*. **2013**, *4*, 2847.
52. Wang, Z.; Liu, B.; Xie, Z.; Li, Y.; Shen, Z. Y.; *Ceram. Int*. **2016**, *42*, 13664.
53. Kumar, A.; Pandey, A. K.; Singh, S. S.; Shanker, R.; Dhawan, A.; *Chemosphere* **2011**, *83*, 1124.
54. Sjogren, J. C.; Sierka, R. A.; *Appl. Environ. Microbiol*. **1994**, *60*, 344.
55. Zuo, X.; Chu, X.; Hu, J.; *Chemosphere* **2015**, *136*, 118.
56. Daikoku, T.; Takemoto, M.; Yoshida, Y.; Okuda, T.; Takahashi, Y.; Ota, K.; Tokuoka, F.; Kawaguchi, A. T.; Shiraki, K.; *Aerosol Air Qual. Res*. **2015**, *15*, 1469.
57. Shiraki, K.; Yamada, H.; Yoshida, Y.; Ohno, A.; Watanabe, T.; Watanabe, T.; Watanabe, H.; Watanabe, H.; Yamaguchi, M.; Tokuoka, F.; Hashimoto, S.; *Aerosol Air Qual. Res*. **2017**, *17*, 2901.
58. Park, D.; Shahbaz, H. M.; Kim, S. H.; Lee, M.; Lee, W.; Oh, J. W.; Lee, D. U.; Park, J.; *Int. J. Food Microbiol*. **2016**, *238*, 256.
59. Kim, S. H.; Shahbaz, H. M.; Park, D.; Chun, S.; Lee, W.; Oh, J. W.; Lee, D. U.; Park, J.; *Innovative Food Sci. Emerging Technol*. **2017**, *39*, 188.
60. Levina, A. S.; Repkova, M. N.; Bessudnova, E. V.; Filippova, E. I.; Mazurkova, N. A.; Zarytova, V. F.; *Beilstein J. Nanotechnol*. **2016**, *7*, 1166.
61. Cui, H.; Jiang, J.; Gu, W.; Sun, C.; Wu, D.; Yang, T.; Yang, G.; *Photochem. Photobiol*. **2010**, *86*, 1135.
62. Kim, J.; Cho, I.; Kim, I.; Kim, C.; Heo, N. H.; Suh, S.; *Rev. Roum. Chim*. **2006**, *51*, 1121.
63. Horovitz, I.; Avisar, D.; Luster, E.; Lozzi, L.; Luxbacher, T.; Mamane, H.; *Chem. Eng. J*. **2018**, *354*, 995.
64. Choi, S. W.; Shahbaz, H. M.; Kim, J. U.; Kim, D. H.; Yoon, S.; Jeong, S. H.; Park, J.; Lee, D. U.; *Innovative Food Sci. Emerging Technol*. **2017**, *39*, 188.
65. Nakano, R.; Ishiguro, H.; Yao, Y.; Kajioka, J.; Fujishima, A.; Sunada, K.; Minoshima, M.; Hashimoto, K.; Kubota, Y.; *Photochem. Photobiol. Sci*. **2012**, *11*, 1293.
66. Sang, X.; Phan, T. G.; Sugihara, S.; Yagyu, F.; Okitsu, S.; Maneekarn, N.; Muller, W. E.; Ushijima, H.; *Clin. Lab*. **2007**, *53*, 413.
67. Hajkova, P.; Spatenka, P.; Horsky, J.; Horska, I.; Kolouch, A.; *Plasma Processes Polym*. **2007**, 397.
68. Lee, J.; Zoh, K.; Ko, G.; *Appl. Environ. Microbiol*. **2008**, *74*, 2111.
69. Lee, S.; Nakamura, M.; Ohgaki, S.; *J. Environ. Sci. Health, Part A: Environ. Sci. Eng*. **1998**, *33*, 1643.
70. Zan, L.; Fa,W.; Peng, T.; Gong, Z. K.; *J. Photochem. Photobiol., B* **2007**, *86*, 165.
71. Watts, R. J.; Kong, S.; Orr, M. P.; Miller, G. C.; Henry, B. E.; *Water Res.* **1995**, *29*, 95.
72. Jafry, H. R.; Liga, M. V.; Li, Q.; Barron, A. R.; *Environ. Sci. Technol*. **2011**, *45*, 1563.
73. Liga, M. V.; Maguire-Boyle, S. J.; Jafry, H. R.; Barron, A. R.; Li, Q.; *Environ. Sci. Technol*. **2013**, *47*, 6463.
74. Zheng, X.; Shen, Z. P.; Cheng, C.; Shi, L.; Cheng, R.; Dong, J.; *RSC Adv*. **2017**, *7*, 52172.
75. Venieri, D.; Gounaki, I.; Binas, V.; Zachopoulos, A.; Kiriakidis, G.; Mantzavinos, D.; *Appl. Catal., B* **2015**, *178*, 54.
76. Mazurkova, N. A.; Spitsyna, Y. E.; Shikina, N. V.; Ismagilov, Z. R.; Zagrebel'nyi, S. N.; Ryabchikova, E. I.; *Nanotechnol. Russ*. **2010**, *5*, 417.
77. Han, W.; Zhang, P. H.; Cao, W. C.; Yang, D. L.; Taira, S.; Okamoto, Y.; Arai, J. I.; Yan, X. Y.; *Prog. Biochem. Biophys*. **2004**, *31*, 982.
78. Koizumi,Y.; Taya, M.; *Biochem. Eng. J.* **2002**, *12*, 107.
79. Habibi-Yangjeh, A.; Asadzadeh-Khaneghah, S.; Feizpoor, S.; Rouhi, A.; *J. Colloid Interface Sci*. **2020**, *580*, 503.
80. Gorbalenya, A. E.; Baker, S. C.; Baric, R. S.; De Groot, R. J.; Drosten, C.; Gulyaeva, A. A.; Haagmans, B. L.; Lauber, C.; Leontovich, A. M.; Neuman, B. W.; Penzar, D.; Perlman, S.; Poon, L. L. M.; Samborskiy, D. V.; Sidorov, I. A.; Sola, I.; Ziebuhr, J.; *Nat. Microbiol*. **2020**, *5*, 536.
81. Yadav, P. D.; Potdar, V. A.; Choudhary, M. L.; Nyayanit, D. A.; Agrawal, M.; Jadhav, S. M.; Majumdar, T. D.; Shete-Aich, A.; Basu, A.; Abraham, P.; Cherian, S. S.; *Indian J. Med. Res*. **2020**, *151*, 200.
82. Schoeman, D.; Fielding, B. C.; *Virol. J*. **2019**, *16*, 1.
83. Gelderblom, H. R.; *Medical Microbiology*, 4th ed.; University of Texas Medical Branch, Galveston, 1996.

84. Crawford, S. E.; Ramani, S.; Tate, J. E.; Parashar, U. D.; Svensson, L.; Hagbom, M.; Franco, M. A.; Greenberg, H. B.; O'Ryan, M.; Kang, G.; Desselberger, U.; *Nat. Rev. Dis.* **2017**, *3*, 1.
85. Markowska-Szczupak, A.; Ulfig, K.; Morawski, A. W.; *Catal. Today* **2011**, *169*, 249.
86. McCaughey, C.; *Ulster Med. J.* **2010**, *79*, 46.
87. Golmohammadi, R.; Fridborg, K.; Bundule, M.; Valegård, K.; Liljas, L.; *J. Mol. Biol*. **1993**, *234*, 620.
88. Peng, X.; Luo, G.; Wu, Z.; Wen, W.; Zhang, X.; Wang, S.; *ACS Appl. Mater. Interfaces* **2019**, *11*, 41148.
89. Xu, R.; Liu, X.; Zhang, P.; Ma, H.; Liu, G.; Xia, Z.; *J. Wuhan Univ. Technol., Mater. Sci. Ed*. **2007**, *22*, 422.
90. Patil, M. D. R.; *Aayushi Int. Inter. Res. J.* **2020**, *7*, 46.
91. Dales, S.; *Encyclopedia of Virology* **1999**, 247.
92. Ouyang, B.; Dong, Y.; Chou, J. J.; *Structural and Functional Properties of Viral Membrane Protein, Advances in Membrane Proteins*; Springer: Singapore, 2018.
93. Vollenbroich, D.; Özel, M.; Vater, J.; Kamp, R. M.; Pauli, G.; *Biologicals* **1997**, *25*, 289.
94. Nel, A.; Xia, T.; Madler, L.; Li, N.; *Science* **2006**, *311*, 622.
95. Bogdan, J.; Zarzynska, J.; Plawinska-Czarnak, J.; *Nanoscale Res. Lett*. **2015**, *10*, 1.
96. Hu, X.; Mu, L.; Wen, J.; Zhou, Q.; *Carbon* **2012**, *50*, 2772.
97. Badireddy, A. R.; Budarz, J. F.; Chellam, S.; Wiesner, M. R.; *Environ. Sci. Technol*. **2012**, *46*, 5963.
98. Akhavan, O.; Choobtashani, M.; Ghaderi, E.; *J. Phys. Chem. C* **2012**, *116*, 9653.
99. Li, Y.; Zhang, C.; Shuai, D.; Naraginti, S.; Wang, D.; Zhang, W.; *Water Res.* **2016**, *106*, 249.